# Fractal Features based on Differential Box Counting Method for the Categorization of Digital Mammograms

Deepa Sankar, Tessamma Thomas
*Department of Electronics*
*Cochin University of Science and Technology*
*Kochi-682022. Kerala. India*
*E-mail:deepasankar@cusat.ac.in, tess@cusat.ac.in*

## Abstract

*Computer aided diagnostic systems can assist radiologist in detecting breast cancer at an early stage with improved mammogram interpretation efficiency. In this paper, six fractal based features obtained from the fractal dimension computed using differential box counting method, are used for distinguishing between normal mammograms from the cancerous ones. The new fractal feature $f_6$ derived from the modified average image is found to be a better feature for distinguishing between normal, malignant and benign masses and mammograms with microcalcifications. The average values of the new normalized fractal feature for normal, mammogram with microcalcifications, benign and malignant tumors are obtained as 0.125, 0.4737, 0.2954, and 0.5992 respectively. The area under the Receiver Operating Characteristics (ROC) curve is found to be 0.923. The study is validated using the mammograms obtained from the online Mammographic Image Analysis Society (MIAS) Digital Mammogram database.*

Keywords- Breast Cancer, Malignant and benign masses, Microcalcifications, fractal dimension, fractal features

## 1. Introduction

Breast cancer is the second leading cause of cancer deaths among women today, after lung cancer. Figures by the World Health Organization show that over 1.2 million persons will be diagnosed with breast cancer worldwide in 2010 [1]. According to a study by International Agency for Research on Cancer (IARC), there will be approximately 250,000 new cases of breast cancer in India by 2015. At present, around 100,000 new cases are reported in India yearly [2].

Cancer is a collection of diseases that causes the cells in the body to be modified and grow uncontrollably. Majority types of cancer cells in due course form a lump or mass called a tumor, and are named after the part of the body where the tumor start offs. Breast cancer originates in breast tissue, which is made up of milk producing glands called lobules, and the ducts that connect lobules to the nipple. The remaining part of the breast is made up of fatty, connective, and lymphatic tissue [3].

Breast cancer can be cured completely when it is detected at an early stage. The survival rate of the patients is 30% higher if it is detected in the initial stage. X ray mammography is an efficient, noninvasive means of examining the breast for detecting breast cancer. Breast tumors and masses appear in the form of dense regions in mammograms. Benign masses generally possess smooth, round and well circumscribed boundaries, while malignant tumors have spiculated, rough and blurry boundaries. In addition, subtle texture differences have been observed between benign and malignant masses with former being mostly homogeneous and the later showing heterogeneous textures [4].

A microcalcification is a tiny calcium deposit that has accumulated in the tissue of the breast and it appears as a small bright spot in the mammogram. These microcalcifications are very difficult to detect because of their small size (typically in the range of 0.05-1mm).Moreover, they are embedded in the non-homogenous mammographic background consisting of overlapping projections of anatomical structures thus making them difficult to detect even for an experienced radiologist.

Figure1 shows the different types of mammograms like normal mammogram and mammogram with microcalcifications, malignant mass and benign mass. Because of the subtle and complex nature of the radiographic findings associated with breast cancer, errors in radiological diagnosis can be attributed to human factors such as varying decision criteria, distraction by other image features, and simple oversight.

Cancerous tumors exhibit a certain degree of randomness associated with their growth, and are typically irregular and complex in shape; therefore, fractal analysis can provide a better measure of their complex patterns than the conventional Euclidean geometry.

But, the breast tissues have similar structures and the regions of normal tissues and abnormal regions have a little difference in contrast, therefore it is very difficult to
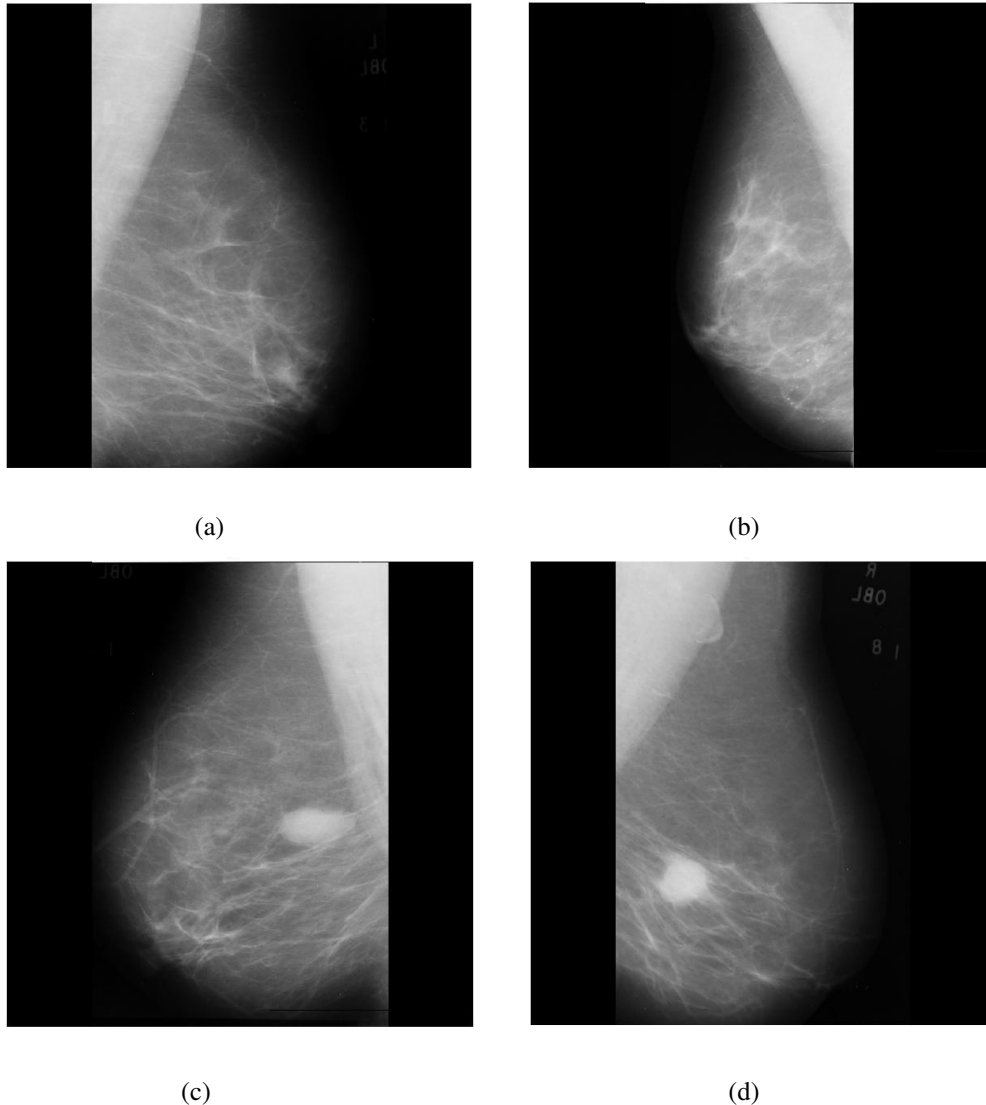
(a)

(b)

(c)

(d)

Figure 1 Different types of mammograms (a) Normal Mammograms (b) Mammogram with Microcalcifications (c) With Benign Mass (d) With Malignant Mass

interpret these images even for an experienced radiologist. In order to increase diagnostic efficiency, computer-assisted schemes based on advanced image processing and pattern recognition techniques can be used to locate and classify possible lesions, thereby alerting the radiologist to examine these areas with particular attention. Moreover, these computer-assisted schemes can improve the performance of the automatic computer-aided diagnosis systems, which can serve as a pre reader" to the radiologist and give the radiologist a "second opinion" in the diagnosis.

Several computer aided techniques have been developed to assist doctors to improve the efficiency and accuracy of mammographic screening programs [5]-[9].

An adaptive mammographic image enhancement method based on the first derivative operators and local statistics features was proposed in [5] to improve the visibility of low-contrast features while suppressing the noises. In [6] an algorithm that combines several artificial intelligent techniques like fractal dimension analysis, multiresolution markov random field, dogs-and-rabbits algorithm etc. with the discrete wavelet transform (DWT) for detection of masses in mammograms is presented. An approach for detecting microcalcifications in mammograms using wavelets, by decomposing the mammograms into different frequency subbands, suppressing the low-frequency subband, and reconstructing the mammogram from the subbands containing only high frequencies is presented in

[7]. Sameti *et.al.* [8] Extracted and analyzed image features from screening mammograms taken prior to the detection of a malignant mass for early detection of breast cancer. Three different pixel-based mass detection methods based on convolution of a mammogram with the Laplacian of a Gaussian, correlation with a model of a mass and statistical analysis of gradient-orientation maps are presented in [9]. In [10] texture and shape features along with the multilayer back propagation neural network with ant colony optimization and particle swarm optimization were used to classify and identify the stages of cancer with an accuracy of 99.5% is presented. Discrimination of benign and malignant mass lesions were done by analyzing the effect of pixel resolution on texture features computed using gray level co-occurrence matrix is presented in [11].

In this paper, features derived from fractal dimension are used to distinguish between different types of breast abnormalities, that is, mammograms with microcalcifications, benign and malignant tumors.

The concept of fractal is used to describe objects that possess self similarity at all scales and levels of magnification [12]. Fractal objects have irregular shapes and complex structures that cannot be represented adequately by the traditional Euclidian dimension. Fractal dimension (FD) assigns non integral dimension values to objects that do not fit to the traditional Euclidean space of objects. For example, the dimension of a straight line is unity, but the dimension of a jagged line is a fractional value falling between unity and two, depending on its degree of jaggedness .The fractal dimension has been used in image classification to measure surface roughness where different natural scenes such as mountains, clouds, trees, and deserts generate different fractal dimensions.

The concept of fractal dimension is given in section II and section III describes the differential box counting method of estimating the fractal dimension. Different fractal features derived from the fractal dimension are explained in section IV while section V gives the results and discussions. Conclusions are given in section VI.

## 2. Fractal Dimension

The concept of fractal dimension is used as an indicator of surface roughness. For a fractal set the Hausdorff- Besicovitch dimension is greater than its topological dimension. Fractal dimension can be used in a large number of applications including image analysis, classification pattern recognition, segmentation etc.

A comparative analysis of the box-counting and ruler methods was used to compute the fractal dimension of both the two-dimensional (2D) contours of breast masses and tumors, as well as their one-dimensional (1D) signatures in [13]. As the fractal dimension of a waveform represents a powerful tool for transient detection, variety of algorithms are available for the computation of fractal dimension. In ref [14], the most common methods of estimating the fractal dimension of biomedical signals directly in the time domain are analyzed and compared. H. Potlapalli el.al describes in [15] a new fractal model based on fractional Brownian motion for texture classification which is invariant to changes in incident light. Brownian motion is particularly useful for outdoor applications, where the viewing direction may change. Determination of the fractal dimension based on the concept of fractional Brownian motion was discussed in [16] with two applications such as classification and edge enhancement of medical images like ultra sound liver images.

Pentland [17] noticed that the fractal model of imaged three dimensional surfaces can be used to obtain shape information and to distinguish between a smooth and rough surface. Two new methods for estimating fractal dimension are introduced in [18], named as wavelet energy fractal dimension and morphological fractal dimension and found that they could be used in image feature extraction and segmentation. Fractal dimension calculated by performing a series of dilations on the three dimensional surface, helped in finding the structural information and gave a robust texture measure of trabecular bone structures in [19]. Ref [20] present a study of four methods to compute the fractal dimension of the contours of breast masses, including the ruler method and the box counting method applied to 1D and 2D representations of the contours and these methods were applied to the contours of breast masses.

Several approaches have been developed to estimate the fractal dimension of images. Of the wide variety of methods for estimating the fractal dimension that have so far been proposed, the box-counting method is one of the more used widely [12], as it can be computed automatically and can be applied to patterns with or without self-similarity.

The box counting method consists in partitioning the image space into square boxes of equal size. The box covers the image space of the function or pattern of interest and the number of boxes that contain at least one pixel of the function is counted. The process is repeated with different box sizes. The fractal dimension is obtained from the slope of the best fitting straight line to the graph plotting the log of the number of boxes counted versus the log of the magnification index for every stage of partitioning as shown in figure2.

For example, an image measuring size M x M pixels is scaled down to s x s, where $1 < s < M/2$, and s is an integer. Then, $r = s/M$ .

Fractal dimension D is given by,

$$D = \frac{\log (N_r)}{\log \left( \frac{1}{r} \right)} \qquad (1)$$

When box counting dimension was used to calculate the fractal dimension of mammograms, and it is observed that there is not much difference in the FD values of normal and abnormal mammograms. Therefore in this paper the differential box counting method is used to calculate the FD and then different fractal features are derived from this fractal dimension.

## 3. Differential Box Counting Method

N. Sarkar and Chaudhuri had proposed the differential box counting (DBC) method and have compared it with other conventional four methods in [21].

Consider an image of size M x M pixels. Let it be scaled down to a size s x s where M/2 > s >1, where s is an integer. Then, r = s/M. Now consider the image to be in a 3D space with (x, y) denoting the spatial co-ordinates, while the z axis denotes the gray level. The (x, y) space is partitioned into grids of size s x s. On each grid there is a column of boxes of size s x s x s'. Figure 2 shows the schematic for computing FD using differential box counting method.

If the total number of gray level is G, then $\lfloor G/s' \rfloor = \lfloor M/s \rfloor$. Numbers from 1, 2... are assigned to the boxes starting from the lowest gray level value. Let the minimum and the maximum gray level of the image in the $(i, j)^{th}$ grid fall in box number k and l, respectively. The contribution of Nr in $(i, j)^{th}$ grid is given by:

$$n_r (i, j)=l – k + 1. \qquad (2)$$

Due to the differential nature in computing $n_r$ this method is called differential box counting method. The contributions from all grids are found by:
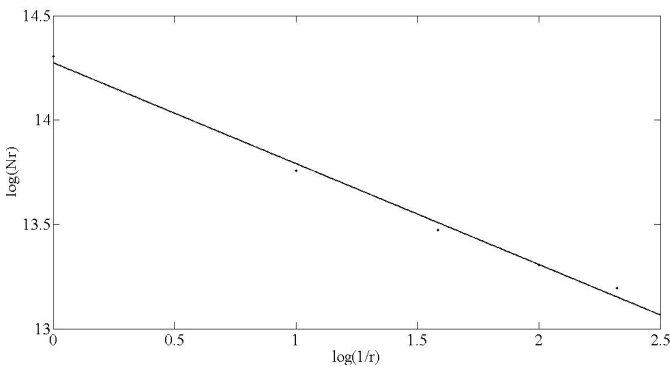
$$N_r = \sum_{i, j} n_r (i, j) \qquad (3)$$



Figure 2. Plot of log (Nr) versus log (1/r)

$N_r$ is computed for different values of s i.e. different values of r. Using equation (1) D, the fractal dimension can be estimated, from the least square linear fit of log $(N_r)$ along log (1/r). The slope of the best fitting curve will give the fractal dimension. Figure 2 shows the plot of log (Nr) versus log (1/r) from which the FD is computed. A random placement of boxes is applied in order to reduce quantization effects.

## 4. Fractal Features

Different textures may have the same fractal dimension. This may be due to combined differences in coarseness and directionality i.e. dominant orientation and degree of anisotropy. Five features derived from [22] based on fractal dimension which are used in this paper are the FD of original image, high gray valued image, low gray valued image, horizontally smoothed image and vertically smoothed image. In addition to these features a new fractal feature is derived from the average of four pixels of the image.

### 4.1 Feature1 ($f_1$)

The FD of the original image is computed on overlapping windows of size (2W + 1) x (2W + 1). Thus, at point (i, j) the first feature value $F_1(i, j)$ is defined as

$$F_1(i, j) = FD\{I_1(i +l, j + k); -W \le l, k \le W\} \qquad (4)$$

where FD is the differential box counting fractal dimension described in section 3. Since the fractal dimension is greater than the topological dimension, the value of $F_1$ is between 2 and 3. The normalized feature is defined as

$$f_1 = F_1(i, j) - 2, \qquad (5)$$

such that $0 \le f_1 \le 1$. Thus all the normalized fractal features are between 0 and 1.

### 4.2 Features 2 and 3 ($f_2$ and $f_3$)

The two modified images called high and low gray-valued images $I_2$, and $I_3$, respectively are defined as:

$$I_2 (i, j) = \begin{cases} I_1 (i, j) – L_1, \text{if } I_1 (i, j) > L_1 \\ 0 \qquad \text{otherwise} \end{cases} \qquad (6)$$

$$I_3 (i, j) = \begin{cases} 255 – L_2, \text{if } I_1 (i, j) > (255 – L_2) \\ I_1 (i, j) \qquad \text{otherwise} \end{cases} \qquad (7)$$

Where

$$L_1 = g_{min} + av/2; \qquad (8)$$

$$L_2 = g_{max} - av/2;$$

with $g_{max}$, $g_{min}$ and av denoting the maximum, minimum and average gray value in $I_1$, respectively. If two images $I_1$, and $J_1$, have a same FD, their high gray-valued images $I_2$ and $J_2$ may not have an identical roughness and their FDs would be different. The same holds for $I_3$ and $J_3$. The normalized features $f_2$ and $f_3$ are computed from $I_2$, and $I_3$ similar to the computation of $f_1$ from $I_1$.

### 4.3 Features 4 and 5 ($f_4$ and $f_5$)

Roughness of an image is directly related to its fractal dimension and therefore its value will be reduced by gray value smoothening. For a highly oriented texture, the FD will be affected least, if the texture is smoothed along the direction of its dominant orientation. But when the smoothing direction is perpendicular, the FD will be considerably reduced. While, a texture is having low degree of anisotropy, it will show an identical effect on the FD, irrespective of the smoothing direction.

Images can be smoothed in the horizontal and vertical direction as:

$$I_4(i, j) = \frac{1}{2w + 1} \sum_{k=-w}^{w} I(i, j + k) \tag{9}$$

$$I_5(i, j) = \frac{1}{2w + 1} \sum_{k=-w}^{w} I(i + k, j) \tag{10}$$

The normalized FD features $f_4$ and $f_5$ are computed similar to $f_1$.

### 4.4 Feature 6 ($f_6$)

A new fractal feature is derived from the smoothened image obtained by computing the average of four neighboring pixels. The new smoothened image is:

$$I_6(i, j) = \frac{1}{4} \sum_{i=1}^{2} \sum_{j=1}^{2} I(i, j) \tag{11}$$

The fractal feature $f_6$ is calculated similar to the previous cases. Authors have found that $f_6$ is a better feature for distinguishing mammograms in [23]

## 5. Results and Discussions

The method proposed in this paper is validated using the digital mammograms obtained from the freely available database provided by the Mammographic Image Analysis Society (MIAS) Digital Mammogram Database [24]. Films taken from the UK National Breast Screening Programme have been digitized to 50 micron pixel edge with a Joyce-Loebl scanning microdensitometer, a device

linear in the optical density range 0 - 3.2. The size of the images in the database is 1024x1024 with 256 gray levels and has a resolution of resolution of 50 micron per pixel. The accompanied 'Ground Truth' contains details regarding the character of the background tissue, class and severity of the abnormality and x, y co-ordinate of its center and radii. In some images calcifications are widely distributed throughout the image rather than concentrated at a single site.

As per the reference [25] the subtlety rating of these mammograms are found to be 1,2 and 3, which indicates that the lesions are detectable only by an expert mammographer, likely to be detected by an expert and likely to be detected by observer with good mammographic training respectively.

For this research, the available 28 mammograms with microcalcifications and 35 each from normal, mammograms with benign and malignant categories were used. The region of interest (ROI) of size 64x 64, 128 x 128, 256 x 256 or 512x512 where chosen from the original image containing microcalcification, benign masses and malignant masses based on the size of the abnormalities present in the mammogram. For normal mammograms also these ROI were considered for the analysis.

While calculating the different features $f_1 – f_6$, overlapping windows of different sizes were used and window of W=2, gave good results.

The different fractal feature images obtained for the mammogram with malignant mass, that is mdb028, are given in figure 3. These images are obtained by applying the equations (4), (6), (7), (9), (10) respectively on the original image. In the feature 3 image it is seen that the information content is lost and therefore the amount of information is less. So the features obtained for this feature are less for all categories of mammograms.

Table 1 shows the mean and standard deviation of the values of the fractal features obtained from the different fractal feature images. The last column in the table shows the new fractal feature $f_6$ obtained for the different categories of the mammograms and is indicated in bold letters. For normal mammograms the complexity is very less. The fractal dimension is an indication of the surface roughness therefore the fractal dimension values and hence the feature values are usually low for normal mammograms. As the presence of cancerous tissues in the breast increases, the complexity and hence the roughness in the mammogram is increased.

For the feature $f_1$, mammograms with microcalcifications gave the highest mean feature value. The average feature value of the normal and malignant masses is found to be in the same range and the least values are obtained for the mammograms with benign masses. The standard deviation of these values shows that
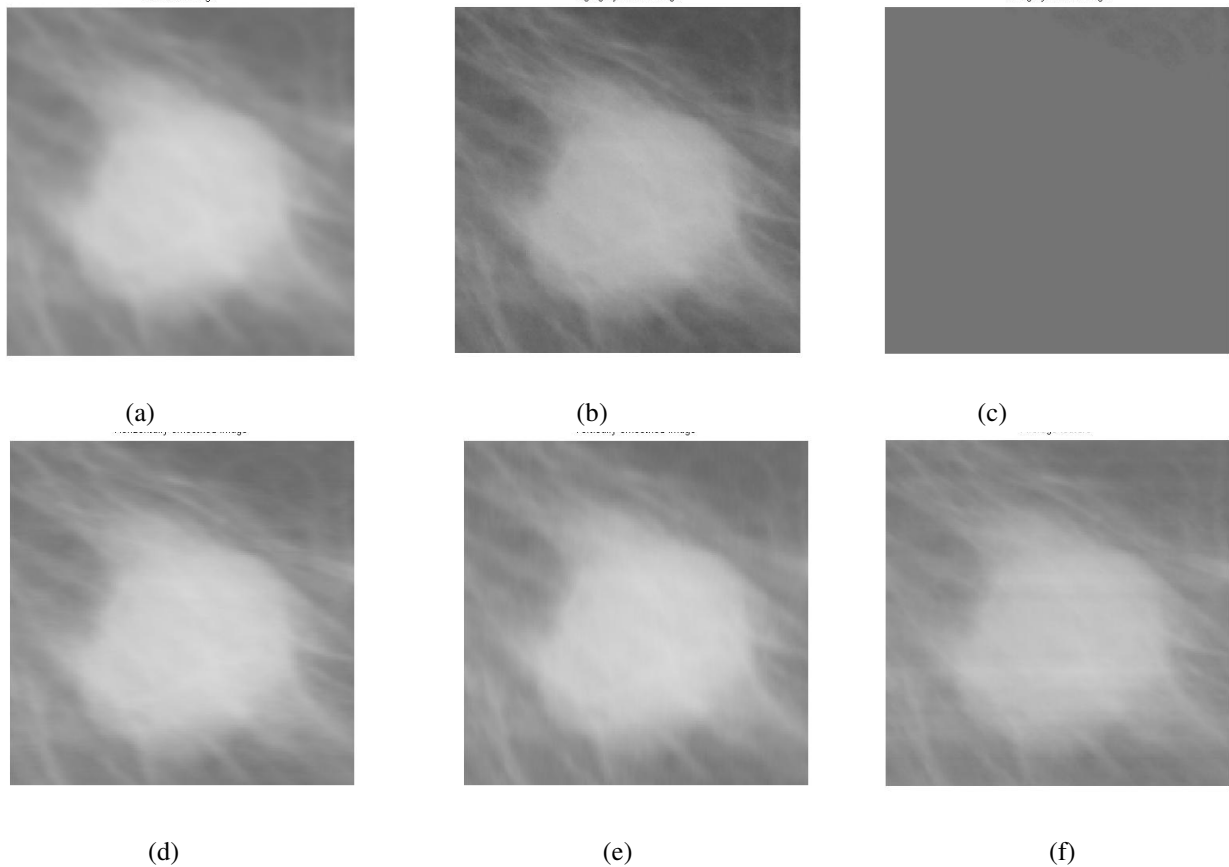
(a)                                    (b)                                    (c)



(d)                                    (e)                                    (f)

Figure 3 Different feature, $f_1$-$f_6$ , images for the mammogram with malignant mass (mdb028)

there is overlap between the values of the different categories of mammograms.

The normal and benign masses had the same range of fractal feature $f_2$ values and similarly that of microcalcifications and malignant masses were in the same range. There is overlap between the individual values of the different categories of the mammograms for $f_2$ also.

As seen in the figure 3, the fractal feature $f_3$ image has the least information and the image is becoming smoother than the original image. The lowest range of the feature $f_3$ is obtained for benign masses and mammograms with microcalcifications. Again all the features values are overlapping for the different classes and are found to be the least distinguishable among all the fractal features calculated.

With feature $f_4$, the highest mean value is obtained for the malignant mass, but the standard deviation indicates that these values overlap with the values of mammograms with microcalcifications category. Using this feature $f_4$, normal mammograms can be distinguished from the ones with microcalcifications and malignant masses.

When the mammograms is vertically smoothed to find feature $f_5$, the feature values of normal and with benign

masses are found to be in the same range. Also, microcalcifications and malignant masses gave similar $f_5$ values.

The new fractal feature $f_6$ is found from the modified image obtained from the average of the four pixels. The values obtained for the different classes of mammograms illustrate that they can be used to differentiate between the different classes of mammograms. The mean feature $f_6$ value of the malignant mass is found to be the highest 0.5992 as expected. The standard deviation of these values is found to be 0.0122. The next higher values are obtained for mammograms with microcalcifications 0.4737 and its standard deviation is 0.0475. Benign masses which appear to be smoother than the microcalcifications gave the average feature value of 0.2954. The least feature values are obtained for the normal mammograms which had rather regular structure and it is found to be 0.125.

The Receiver Operating Characteristics (ROC) analyses were done to compare the performance of these features to distinguish the different mammograms. The plot of the ROC curves is given in figure 4. An ROC curve was generated by using a sliding threshold on the selected feature and computing the sensitivity and

Table 1 Comparison of the different fractal features obtained for normal mammograms, mammograms with Microcalcification and Benign and Malignant masses

| Mammo-grams | Fractal Features | | | | | | | | | | | |
|---|---|---|---|---|---|---|---|---|---|---|---|---|
| | $f_1$ | | $f_2$ | | $f_3$ | | $f_4$ | | $f_5$ | | $f_6$ | |
| | *Mean* | *Std dev* | *Mean* | *Std dev* | *Mean* | *Std dev* | *Mean* | *Std dev* | *Mean* | *Std dev* | *Mean* | *Std dev* |
| *Normal* | 0.2042 | 0.0317 | 0.283 | 0.0587 | 0.2159 | 0.0857 | 0.242 | 0.0739 | 0.226 | 0.0655 | **0.125** | **0.0243** |
| *Benign* | 0.1529 | 0.0739 | 0.227 | 0.049 | 0.1412 | 0.0744 | 0.3181 | 0.0875 | 0.2894 | 0.0888 | **0.2954** | **0.0317** |
| *With Microcal-cifications* | 0.3559 | 0.0685 | 0.3141 | 0.0947 | 0.1991 | 0.1119 | 0.4279 | 0.0924 | 0.4324 | 0.081 | **0.4737** | **0.0475** |
| *Malignant* | 0.2884 | 0.0709 | 0.3104 | 0.0765 | 0.2259 | 0.0808 | 0.4662 | 0.1442 | 0.4447 | 0.0147 | **0.5992** | **0.0122** |

specificity for each threshold. The true-positive fraction (TPF), or sensitivity, is the proportion of the abnormal cases correctly identified by the feature. The false-positive fraction (FPF), is the proportion of the normal cases incorrectly identified by the classifier as abnormal. The TPF and the FPF are plotted to yield the ROC curve. The Area under the ROC curve (AUC) for the feature $f_1$, is found to be 0.67 and had a 95%confidence interval of 0.54 to 0.835. The z statistics of this feature is obtained as 2.408.
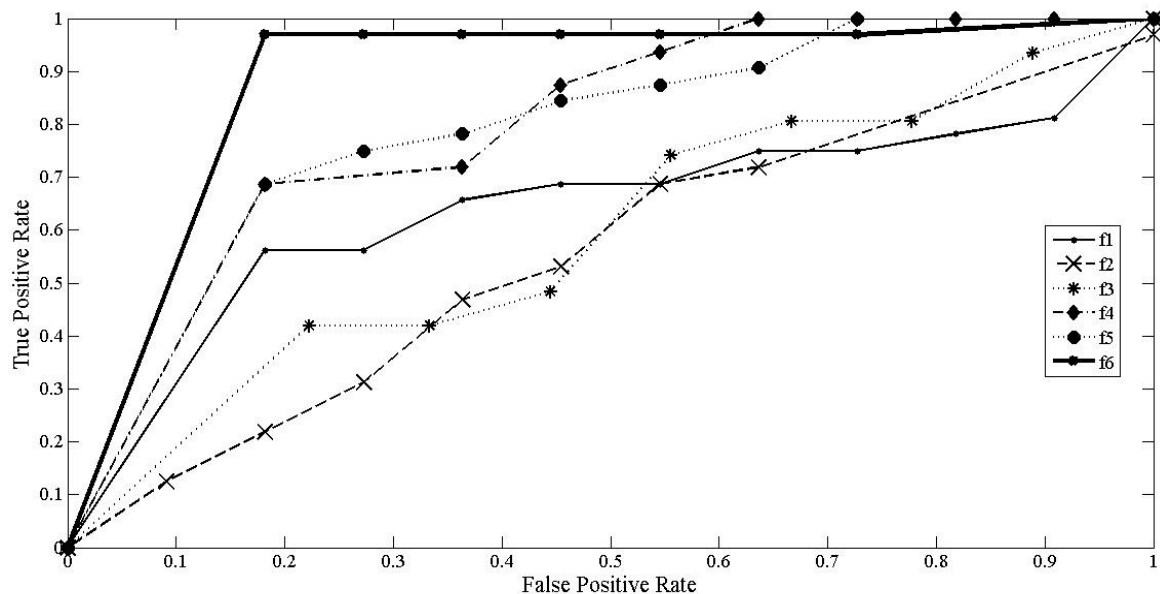


Figure 4 Receiver Operating Characteristics Curves for the different fractal features

The AUC, CI and z statistics of $f_2$ was obtained as 0.56, 0.32% to 0.67% and 1.605 respectively. For feature $f_3$, AUC was found to be 0.523, 95%CI was 0.438 to 0.743 and z statistics value of 1.035. AUC values are found to be the least for this feature and cannot discriminate between the different mammograms. AUC of feature $f_4$ is obtained as 0.866 with a 95% confidence interval between 0.728% to 0.95%. The z statistic of $f_4$ is 5.64 AUC of the feature $f_5$ was found to 0.722 with a z statistics of 4.38. The 95 % confidence interval was obtained to be between 0.65% to 0.93%. The highest AUC is obtained for the new feature f6 of 0.923. The CI and z statistics are 0.855% to 0.967% and 15.62 respectively.

## 6. Conclusions

Different fractal features used for analyzing mammograms based on fractal dimension computed using the differential box counting method are compared in this paper. A new fractal feature estimated from the modified smoothed image by computing the average of four neighboring pixels. It is found that this feature $f_6$ can obviously distinguish between normal, mammograms with microcalcifications, benign masses and malignant tumors. From the table1 it is clear that the malignant tumors whose roughness is high are having the highest value compared to the other types. For the feature $f_6$, the values increases as roughness increases from normal, to benign to microcalcifications to malignant tumors.

For the other features there is overlap among the individual values of the different types of mammograms. Also it is seen that the feature $f_3$ is least suited for discriminating the mammograms. The standard deviation indicates the values obtained are close to the average value and the dispersion of the values from the mean is very less. Once the features are selected these can be used for the classification of normal, benign, malignant and mammograms with microcalcifications.

The ROC analysis of these features also shows that the highest Area under the ROC curve, 0.923, is obtained for this feature. There is overlap in certain individual values but this can be overcome if more features are included in the system.

## 7. References

[1] http://www.healthinformations.info/2010/03/ breast-cancer-statistics-how-breast.html (accessed April 2010)

[2] http://www.thaindian.com/newsportal/health/breast-cancer-will-become-epidemic-in-india-oncology-pioneer _10037691. html (accessed April 2010)

[3] American Cancer Society –Breast Cancer Fact and Figures 2009-2010 website: http://mdproacs01-vip0.usi.net/downloads/STT/ F86 1009_final%209-08-09.pdf (accessed April 2010)

[4]Tingting Mu,Asoke K. Nandi, Rangaraj M. Rangayyan2, "Classification of Breast Masses Using Selected Shape, Edge-sharpness, and Texture Features with Linear and Kernel-based Classifiers", Journal of Digital Imaging, Vol 21, No 2 (June), 2008: pp 153-169

[5] Jong Kook Kim, Jeong Mi Park, Koun Sik Song, Hyun Wook Park, "Adaptive Mammographic Image Enhancement Using First Derivative and Local Statistics", IEEE Transactions on Medical Imaging, Vol. 16, No. 5, October 1997, pp.495-502

[6] Lei Zheng, Andrew K. Chan, "An Artificial Intelligent Algorithm for Tumor Detection in Screening Mammogram", IEEE Transactions on Medical Imaging, Vol. 20, No. 7, July 2001, pp. 559-567

[7] Ted C. Wang , Nicolaos B. Karayiannis "Detection of Microcalcifications in Digital Mammograms Using Wavelets", IEEE Transactions on Medical Imaging, Vol. 17, No. 4, August 1998, pp 498 – 509

[8] Mohammad Sameti, Rabab Kreidieh Ward, Jacqueline Morgan-Parkes, Branko Palcic , "Image Feature Extraction in the Last Screening Mammograms Prior to Detection of Breast Cancer", IEEE Journal of Selected Topics in Signal Processing, Vol. 3, No. 1, February 2009,pp.49-52

[9] Guido M. te Brake, Nico Karssemeijer, "Single and Multiscale Detection of Masses in Digital Mammograms", IEEE Transactions on Medical Imaging, Vol. 18, No. 7, July 1999, pp.628-639

[10] Muthusamy Suganthi, Muthusamy Madheswaran "An Improved Medical Decision Support System to Identify the Breast Cancer Using Mammogram", Journal of Medical Systems, Springer Netherlands, available online March 2010 DOI: 10.1007/s10916-010-9448-5

[11] Rangaraj M Rangayyan, Thanh M Nguyen, Fabio J Ayres, Asoke K Nandi , "Effect of pixel resolution on texture features of breast masses in mammograms", Journal of Digital Imaging, Springer New York, Published online 12 September 2009,DOI : 10.1007/s10278-009-9238-0

[12] Benoit B Mandelbrot, "The Fractal Geometry of

Nature", W.H.Freeman and Company,NewYork,1983

[13] T.M. Nguyen, Rangaraj M. Rangayyan, "Shape Analysis of Breast Masses in Mammograms via the Fractal Dimension", Proceedings of the 2005 IEEE Engineering in Medicine and Biology, Shanghai, China, September 1-4, 2005 pp-3210-3213

[14] Rosana Esteller, George Vachtsevanos, Javier Echauz, Brian Litt, "A Comparison of Waveform Fractal Dimension Algorithms", IEEE Trans. On Circuits and Systems -I: Fundamental Theory and Applications, Vol. 48, No. 2, pp 177-183 Feb 2001.

[15] Harsh Potlapalli , Ren C. Luo, " Fractal-Based Classification of Natural Textures", IEEE Trans. On Industrial Electronics, Vol. 45, No. 1, pp 142-150,Feb 1998.

[16] C.-C. Chen, J. S. Daponte, M. D. Fox, "Fractal feature analysis and classification in medical imaging," IEEE Trans. Med. Imag., vol. 8, pp.133–142, June 1989.

[17] P. Pentland, "Fractal-based description of natural scenes," IEEE Trans. Pattern Anal. Machine Intell., vol. PAMI-6, pp. 661–674, Nov. 1984.

[18] Yuxin Liu,  Yanda Li ," Image Feature Extraction and Segmentation using Fractal Dimension", Proc. of the International Conference on Information, Communications and Signal Processing ICICS '97, pp.975-979,  Singapore, 9-12 September 1997

[19] J. Samarabandu, R. Acharya, E. Hausmann, K. Allen, "Analysis of   Bone X-Rays Using Morphological Fractals", IEEE Trans. on Medical Imaging, Vol. 12, No. 3, Sep. 1993.

[20] Rangayyan RM, Nguyen TM,  "Fractal analysis of contours of breast masses in mammograms", Journal of Digital Imaging,  Vol- 20, No.3, pp-223–237, 2007.

[21] Nirupam Sarkar,  B. B. Chaudhuri, "An Efficient Differential Box-Counting Approach to Compute Fractal Dimension of Image", IEEE Trans. on Systems, Man and Cybernetics, Vol. 24, No. 1. Jan 1994, pp-115-120

[22] B. B. Chaudhuri , Nirupam Sarkar , "Texture Segmentation Using Fractal Dimension", IEEE Transactions on Pattern Recognition and Machine Intelligence, Vol. 17, No. 1, Jan 1995

[23] Deepa Sankar, Tessamma Thomas, "Analysis of Mammograms using Fractal Features", Proc. of the  8th International Conference on Computer Information Systems and Industrial Management Applications (CISIM 2009), December 09-11, 2009, Coimbatore, India,pp.936-941.

[24] J Suckling  et al (1994):  The Mammographic Image Analysis Society Digital Mammogram Database Exerpta Medica International Congress Series 1069 pp375-378

[25] Etta D. Pisano, "Breast Imaging", IOS Press,1998